



A Journal of



Accepted Article

Title: Synthesis and photochemical properties of Mn(I) tricarbonyl diimine complexes bound to tetrazolato ligands

Authors: Matthew Stout, Alessandra Stefan, Brian Skelton, Alexandre Sobolev, Massimiliano Massi, Alejandro Hochkoepler, Stefano Stagni, and Peter Simpson

This manuscript has been accepted after peer review and appears as an Accepted Article online prior to editing, proofing, and formal publication of the final Version of Record (VoR). This work is currently citable by using the Digital Object Identifier (DOI) given below. The VoR will be published online in Early View as soon as possible and may be different to this Accepted Article as a result of editing. Readers should obtain the VoR from the journal website shown below when it is published to ensure accuracy of information. The authors are responsible for the content of this Accepted Article.

To be cited as: *Eur. J. Inorg. Chem.* 10.1002/ejic.201900987

Link to VoR: <http://dx.doi.org/10.1002/ejic.201900987>

WILEY-VCH

Synthesis and photochemical properties of Mn(I) tricarbonyl diimine complexes bound to tetrazolato ligands

Matthew J. Stout,^[a] Alessandra Stefan,^[b,c] Brian W. Skelton,^[d] Alexandre N. Sobolev,^[d] Massimiliano Massi,^{*[a]} Alejandro Hochkoepler^[b,c], Stefano Stagni,^[e] Peter V. Simpson^{*[a]}

Abstract: Ten manganese(I) tricarbonyl diimine complexes bound to variably functionalised 5-aryl-tetrazolato ligands were prepared, and their photochemical properties were investigated. Upon exposure to light at 365 nm, each complex decomposed to its free diimine and tetrazolato ligands, simultaneously dissociating three CO ligands, as evidenced by changes in the IR spectra of the irradiated complexes over time. The anti-bacterial properties of one of these complexes were tested against *Escherichia coli*. While the complex displayed no effect on the bacterial growth in the dark, pre-irradiated solutions inhibited bacterial growth. Comparative studies revealed that the antibacterial properties originate from the presence of free 1,10-phenanthroline.

Introduction

Carbon monoxide is a very important intracellular signalling molecule. It is endogenously produced at low concentrations following the breakdown of free haemoglobin by the enzyme family haem oxygenases (HOs), as a response to tissue damage.^[1-4] Consequently, many studies have been conducted on the therapeutic properties of administered exogenous CO, demonstrating beneficial effects such as anti-inflammation, tissue protection, anti-cancer, and anti-bacterial.^[5-10] However, due to the high toxicity of CO and lack of spatial specificity, administering CO as an inhaled gas presents some significant drawbacks.^[11] Early research in this field by Motterlini and co-workers^[12] addressed this problem by preparing the very first carbon

monoxide releasing molecules (CORMs) to release CO endogenously within the body, including the first photoactivated CORM (photoCORM), dimanganese decacarbonyl (referred to as CORM-1). CORM-1 was the first evidence that a transition metal carbonyl complex could potentially act as a carrier to deliver CO. However, it lacked solubility in aqueous media, was highly toxic and required harmful UV light for activation.^[13-14] Since this early research, the field has rapidly expanded with photoCORMs designed for high solubility in biological media, tissue specificity, defined CO release rate, and red-shifted light absorption.^[15-28] Previous research within our group explored the use of luminescent rhenium complexes of the type $\text{Re}(\text{N}^{\wedge}\text{N})(\text{CO})_3\text{L}$, where $\text{N}^{\wedge}\text{N}$ is a diamine-type ligand such as 1,10-phenanthroline and L is a functionalised 5-aryl-tetrazolato ligand, as cellular probes.^[29-32] Our studies indicated that this class of complexes possess suitable properties as building blocks for the preparation of cellular markers with specifically tailored properties, as for example the staining of polar lipids in live cells and tissue. The cytotoxicity to these complexes was quite low, which was ascribed to their inertness towards potential ligand exchange reactions in cells. On the other hand, manganese complexes bound to tetrazolato anions are relatively unexplored, and virtually none of these species have been investigated for biological applications.^[33-36] We therefore envisaged that the corresponding manganese analogues of our previously published rhenium complexes could possess CO-releasing properties and tuning of the biological properties such as organelle targeting.

In this work, we present the synthesis, structural and photochemical characterisation of ten neutral complexes of the type $\text{Mn}(\text{N}^{\wedge}\text{N})(\text{CO})_3\text{L}$. Their photochemical properties have been assessed by a combination of UV-Vis, IR and NMR spectroscopies, revealing decomposition of the species with the simultaneous liberation of three CO ligands. This feature was preliminarily explored to assess inhibition of *Escherichia coli* bacterial growth.

[a] Matthew J. Stout, Assoc. Prof. Massimiliano Massi and Dr Peter V. Simpson

Curtin Institute for Functional Molecules and Interfaces, School of Molecular and Life Sciences, Curtin University, Kent Street, Bentley 6102, Perth, Australia
E-mail: m.massi@curtin.edu.au, peter.simpson@curtin.edu.au

[b] Dr Alessandra Stefan and Assoc. Prof. Alejandro Hochkoepler
CSGI, Department of Chemistry, University of Florence, I-50019 Sesto Fiorentino (FI), Italy

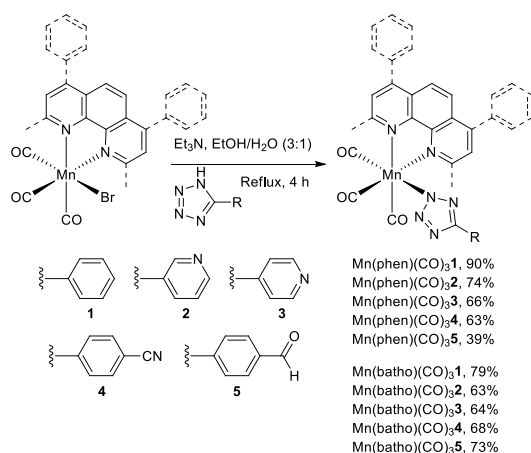
[c] Dr Alessandra Stefan and Assoc. Prof. Alejandro Hochkoepler
Department of Pharmacy and Biotechnology, University of Bologna, Viale Risorgimento 4, I-40136 Bologna, Italy

[d] Prof. Brian W. Skelton and Dr Alexandre N. Sobolev
School of Molecular Sciences and CMCA, the University of Western Australia, 35 Stirling Highway, 6009, Perth, Western Australia

[e] Assoc. Prof. Stefano Stagni
Department of Industrial Chemistry "Toso Montanari", University of Bologna, Viale Risorgimento 4, I-40136 Bologna, Italy

Supporting information for this article is given via a link at the end of the document.

FULL PAPER



Scheme 1. Synthesis of manganese tetrazolate complexes.

Results and Discussion

The preparation of the precursor complexes $\text{Mn}(\text{phen})(\text{CO})_3\text{Br}$ and $\text{Mn}(\text{batho})(\text{CO})_3\text{Br}$ (where phen is 1,10-phenanthroline and batho is bathocuproine), as well as their subsequent reactions with tetrazoles (**1-5H**), were based on a modification of previously published works.^[37-39] The $\text{Mn}(\text{phen})(\text{CO})_3\text{Br}$ and $\text{Mn}(\text{batho})(\text{CO})_3\text{Br}$ precursors were refluxed in the dark with a slight excess of the corresponding tetrazole and triethylamine in a 3:1 ethanol/water mixture. All the complexes were purified following by filtration and subsequent re-precipitation, and were obtained as yellow powders in moderate to high yields. The complexes are soluble in all common organic solvents including acetone, dichloromethane, methanol, acetonitrile, dimethylformamide, and dimethylsulfoxide.

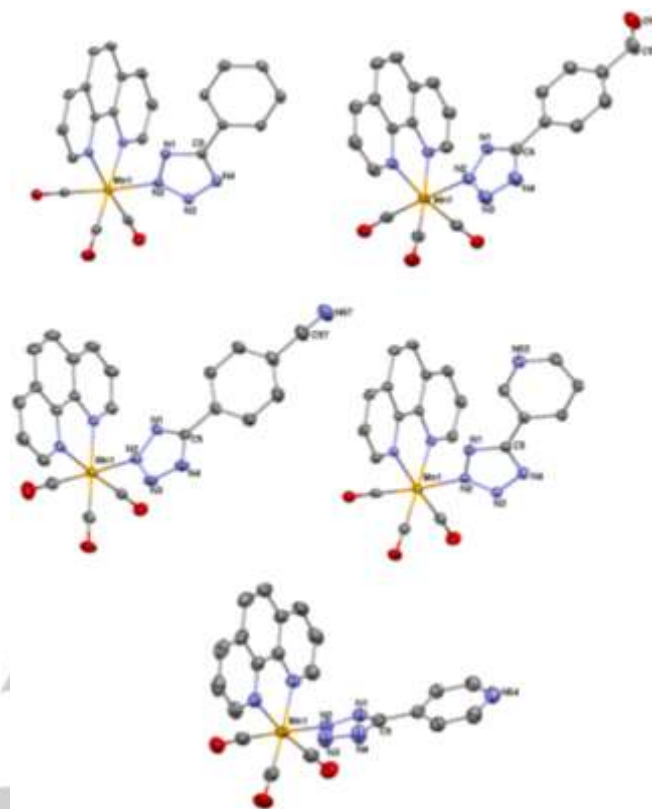


Figure 1. X-ray crystal structures of $\text{Mn}(\text{phen})(\text{CO})_3(\mathbf{1-5})$ with displacement ellipsoids drawn at the 50% probability level. Hydrogen atoms have been omitted for clarity.

The IR spectra of all complexes contained two CO bands, with the lower energy band being the superimposition of two quasi-degenerate peaks, consistently with three carbonyl ligands in a *facial* arrangement. The frequencies of the CO stretching vibrations were very similar for all the complexes, with all of them showing a hypsochromic shift compared to the starting bromo complex. This increase in CO frequency is due to the tetrazolato ligands being a stronger π acceptors compared to the bromo ligand. As a result, the tetrazolato complexes reduce electron density on the Mn(I) centre, translating to a decrease in backbonding from the Mn(I) to the CO ligands and higher CO frequency for the complexes. This behaviour has been previously observed in analogous Re(I) complexes.^[37-39]

The ^1H and ^{13}C NMR spectra of the complexes exhibited the expected number of signals, highlighting the symmetric arrangement of the phen and batho ligands originating from the *facial* configuration of the carbonyl ligands. Further investigation of the complexes by ^{13}C -NMR showed signals between 160–164 ppm for the quaternary carbon of the various tetrazole rings. Based on previous studies on analogous Re(I) complexes, these values suggest coordination of the Mn(I) centres to the N2 atom of the tetrazole ring, as opposed to N1 coordination which would show a more shielded value around 155 ppm.^[37-39]

The single crystal X-ray diffraction structures of complexes $\text{Mn}(\text{phen})(\text{CO})_3(\mathbf{1-5})$ revealed similar structures (Figure 1), where

FULL PAPER

in all cases the Mn centres display a slightly distorted octahedral geometry with to three CO ligands bound in a *facial* arrangement. All the tetrazole ligands are bound through their N2 position in a similar manner to the previously reported rhenium complexes.

The absorption spectra of all complexes recorded from diluted DCM solutions (see Figure 2 for two examples displaying the phen and batho complexes bound to **4**; the remaining absorption spectra are available in the SI) exhibit high energy bands in the 250-350 nm region, and broad featureless bands with lower molar absorptivity between 350 and 500 nm. The high energy bands are attributed to ligand-centred (LC) π - π^* transitions within the phen and batho ligands. On the other hand, the red-shifted broad bands are typical of metal-to-ligand charge transfer (MLCT) transitions from the manganese centre to the phen and batho ligands. The MLCT absorption maxima of the complexes appear in the 350-370 nm region and are blue shifted by around \sim 60 nm when compared to the starting material complexes Mn(phen)(CO)₃Br and Mn(batho)(CO)₃Br (\sim 430 nm).^[40] This blue shift is again consistent with the tetrazole ligands being stronger π -acceptors with respect to bromide, stabilising the 3d orbitals of the manganese centre. No significant shift in MLCT absorption maxima was observed between the Mn(phen)(CO)₃(**1-5**) and Mn(batho)(CO)₃(**1-5**) complexes.

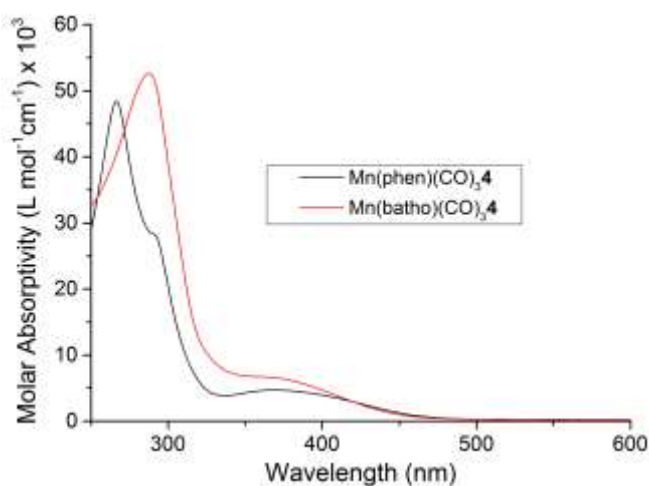


Figure 2. UV-VIS spectra of Mn(phen/batho)(CO)₃**4** from diluted DCM solutions.

When stored in the dark, either in the solid state or in solution (acetone and dichloromethane), the complexes appear to be stable, as verified by the lack of changes in their IR and NMR spectra over time. When exposed to standard ambient illumination within the laboratory, however, the complexes in the solid state changed colour from pale yellow to a mixture of white and brown within a day. This colour change occurred significantly faster when the complexes were dissolved, forming a colourless solution containing a brown precipitate within hours. In order to investigate the photoreaction occurring when the complexes are exposed to light, photolysis experiments were performed by irradiating dichloromethane or acetone solutions containing the complexes with a 365 nm pen lamp source. The irradiated

solutions were then monitored by IR spectroscopy to highlight changes in the carbonyl bands. The simultaneous disappearance of all three CO stretches upon illumination was observed within 25 minutes for all complexes. Using complex Mn(phen)(CO)₃**4** as an example, the presence of CO peaks 2036 and 1942 cm⁻¹ completely collapsed after 25 minutes of photolysis (Figure 3; see SI for the remaining complexes) indicating that no Mn-CO bonds remained. During this transition, the solution went from yellow (0 min) to dark orange (4-16 min), then eventually becoming clear and colourless with the concomitant formation of a dark precipitate (25 min). The absence of visible colour suggests that Mn was no longer bound to phen. During photolysis, the formation of minor sharp bands with weak intensity was observed, tentatively attributed to short-lived intermediate manganese species forming and decomposing during the photolysis, although these intermediates were not completely characterised.

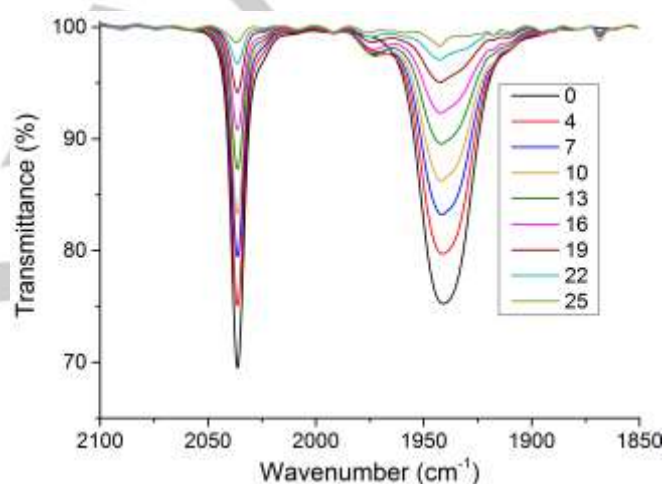


Figure 3. Progressive IR spectra (carbonyl bands region) of a dichloromethane containing the complex Mn(phen)(CO)₃**4** irradiated with a 365 nm pen lamp source. The time intervals presented in the framed legend are expressed in minutes.

A fully photolysed solution of Mn(phen)(CO)₃**4** was analysed using ¹H-NMR to determine the identity of the formed species. Initially, a broad and unresolvable band was observed in the aromatic region of the spectra. It was postulated that Mn(I) had oxidised to a paramagnetic Mn species that caused significant line broadening in the ¹H-NMR spectrum. In addition, each photolysed complex resulted in a clear solution containing a dark brown precipitate. Removal of the dark brown solid produced a spectrum with better defined peaks, albeit still broad in appearance (Figure 4), leading us to postulate that the identity of the dark brown precipitate was manganese dioxide. These broad peaks were directly compared with the spectra of the free phen and the triethylammonium salt of **4** (Figure 4). The signals at 9.11, 8.50, 8.00 and 7.78 ppm matched for free phen, whilst the signals at 8.14 and 7.82 ppm fit with the deprotonated tetrazole ligand.

FULL PAPER

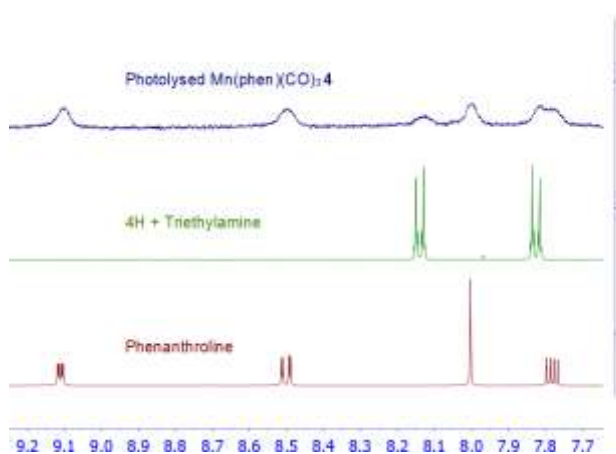


Figure 4. Stacked DMSO- d_6 H-NMR spectra: photolysed solution of Mn(phen)(CO) $_3$ 4 (blue), free 4H and triethylamine (green), free phenanthroline (red).

In order to determine the identity of the excited state where decomposition of the complexes is observed, dichloromethane solutions of Mn(phen)(CO) $_3$ 4 and Mn(batho)(CO) $_3$ 4, used as exemplar for phen and batho containing manganese complexes, were exposed to a range of wavelengths from purple (415 nm) to yellow (555 nm), using a PoliLight FL 500 (Universal Forensic Light) as the source. Figure 5 displays the decrease of intensity of the A $_1$ ' carbonyl band upon irradiation with various wavelengths, normalised to the intensity of the carbonyl band from a solution maintained in the dark (as a ratio of transmittance from photolysed solution, T, and transmittance of solution kept in the dark, T $_i$). The extent of photolysis rapidly decreases when the wavelengths elongate past 490 nm, suggesting that the complexes decompose from MLCT excited states.

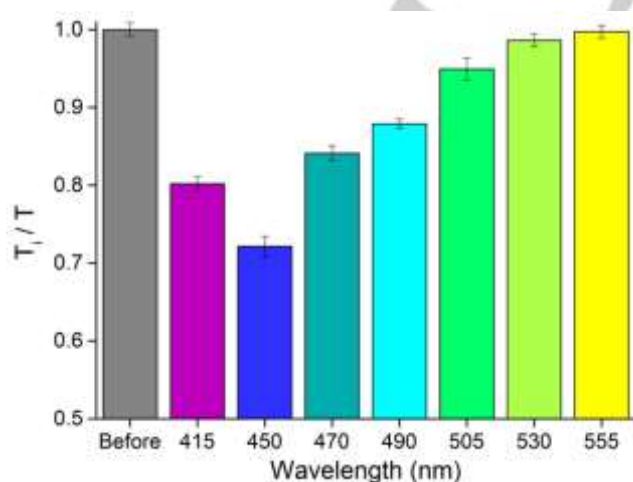
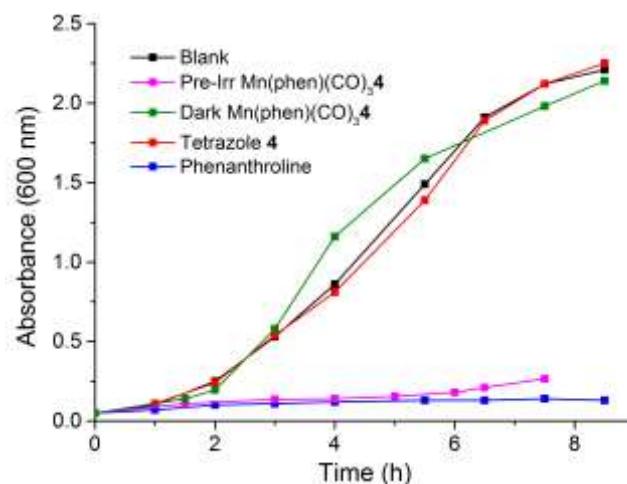


Figure 5. Ratio of initial transmittance (T $_i$) over post photolysis transmittance (T) for the Mn(phen)(CO) $_3$ 4 carbonyl (A $_1$ '). CO release at different wavelengths of irradiation using PoliLight FL 500. The error bars correspond to the standard deviation of three independent measurements.

Mn(phen)(CO) $_3$ 4 was tested for its antibacterial activity against Gram-negative *E. coli*, as photoCORMs have recently been found to be very efficient anti-bacterial agents.^[41-47] A comparative experiment was set up to individually investigate an aqueous solution (1.2% DMSO in H $_2$ O, pH 6.9) of the intact complex (maintained in the dark) and a prefiltered (to remove unknown manganese oxide species) photolysed solution (pre-irradiated with 365 nm until the UV-Vis spectrum did not show any MLCT band). The growth curves obtained were also compared with a blank (1.2% DMSO/LB only) and with aqueous solutions containing only the tetrazole or the phenanthroline ligand, all at a concentration of 100 μ M. The resulting growth curves are shown in Figure 6. The results indicate that while the intact complex does not inhibit *E. coli* growth, the photolysed solution has a strong inhibitory effect with a fully suppression of the bacterial growth. When Mn(phen)(CO) $_3$ 4 was pre-photolysed, *E. coli* growth was completely inhibited at 100 μ M sample concentration, whilst a 5 μ M concentration did not significantly alter the growth rate of *E. coli* (see SI). Subsequent growth curves conducted on free ligands confirmed that tetrazole 4 had no effect on *E. coli* growth at 100 μ M and 5 μ M concentrations whilst phenanthroline completely inhibited bacterial growth similarly to the pre-irradiated Mn(phen)(CO) $_3$ 4 at 100 μ M concentration and slightly decreased the rate of bacterial growth when used at 5 μ M. This result is in agreement with previous research showing antibacterial properties of phen, whose minimum inhibitory concentration (MIC) is reported to be 20 μ g mL $^{-1}$.^[48] To assess whether CO release could potential have a synergistic effect with phen on the bacterial growth, *E. coli* culture were incubated with the complex at 100 μ M and 5 μ M, and then irradiated under the same conditions. However, no significant differences were detected (see SI), suggesting the release of CO in this case did not affect bacterial growth along with phen.



FULL PAPER

Figure 6. *E. coli* growth curves at 37 °C in the presence of 100 μM Mn(phen)(CO)₃4 pre-photolysed or maintained in the dark (pink and green lines, respectively), phenanthroline (blue line) and tetrazole 4 (red line). A control culture containing DMSO alone (1.2%) was prepared (dark line).

Conclusions

A series of ten manganese(I) complexes were synthesised and fully characterised, including X-ray crystal structure analysis for the five complexes bound to the phenanthroline. All compounds are stable in the dark. However, upon excitation to the lowest MLCT manifold, all three carbonyls are lost simultaneously, leading to the release of phen/batho and corresponding tetrazolato ligands. The complexes could be activated with a variety of light source from low power artificial lab light to a high power PoliLight, ranging from wavelengths 365-555 nm. Bacterial growth inhibition was tested for solutions containing either the intact or the photolysed complex, with inhibition of *E. coli* observed for the latter. This effect seems to be caused by the presence of phen species since phenanthroline alone inhibited bacterial growth to a similar level observed in the presence of the pre-irradiated Mn(phen)(CO)₃4.

Experimental Section

General considerations

All reagents and solvents were purchased from Sigma Aldrich, Alfa Aesar and Strem Chemicals and used as received without further purification. All experiments were performed in the dark by wrapping glassware in aluminium foil. All complexes were prepared by modification of previously published procedures.³ Nuclear magnetic resonance spectra were recorded using a Bruker Avance 400 spectrometer (400.1 MHz for ¹H; 100 MHz for ¹³C) at 300 K. All the NMR spectra were calibrated to residual solvent signals. Infrared spectra were recorded using an attenuated total reflectance Perkin Elmer Spectrum 100 FT-IR with a sodium chloride cell. IR spectra were recorded from 4000 to 650 cm⁻¹. Elemental analyses were obtained at Curtin University using a Thermo Finnigan EA 1112 Series Flash. Absorption spectra were recorded at room temperature using a Cary 4000 UV-Vis spectrometer.

Lamp photolysis experiments were carried out using a UVP Blak-Rays B-100AP High Intensity UV lamp with a 100 W bulb at a single wavelength output of 365 nm. The experiments were performed under darkness, the complexes dissolved in dichloromethane (3 mL, 7.8mM) and stored in a quartz cuvette. The distance between quartz and lamp source was kept constant at a 3 cm distance. The lamp was switched off at set intervals and the solutions analysed in a NaCl (5 mm) disc on a Perkin-Elmer Spectrum 2000 FT-IR spectrometer. The range of wavelengths able to activate the complexes were tested using a PoliLight FL 500 Universal Forensic Light. Complexes were dissolved in dichloromethane (3 mL, 7.8 mM) and placed in a quartz cuvette and kept 6 cm away from the PoliLight. Solutions were irradiated for 15 seconds each, and CO loss was measured using a NaCl (5 mm) disc on a Perkin-Elmer Spectrum 2000 FT-IR spectrometer.

Escherichia coli TOP10 strain was streaked from a 20% glycerol stock on Luria-Bertani (LB) agar plates (10 g/L tryptone, 5 g/L yeast extract, 10 g/L NaCl, 15 g/L agar), and grown at 37°C overnight. A single colony was used

to prepare the pre-culture in LB liquid medium. After overnight incubation at 37 °C under shaking (180 rpm), the pre-culture was used to inoculate independent cultures (5 mL of fresh LB) containing different concentrations of Mn(phen)(CO)₃4 dissolved in dimethylsulfoxide/water (50:50). A control culture in absence of any complex containing DMSO alone (1.2 or 0.5%) was also prepared. The growth curve at 37 °C of each *E. coli* culture was obtained by measuring the optical density at 600 nm (OD600) as a function of time using a UV-Vis spectrophotometer.

The synthesis of the manganese complexes was carried out using procedures adapted from previously published works.¹ Complexes were kept under darkness at all times during reaction, work up and storage. The tetrazole ligand (1.1 eq.) and triethylamine (3.0 eq.) were added to a 12 mL ethanol/water mixture (3:1 v/v). The mixture was stirred at room temperature for 15 minutes, followed by the addition of fac-Mn(diim)(CO)₃Br (1.0 eq.). The mixture was then heated at reflux for 4 hours. The resulting yellow solution was reduced in vacuo and 20 mL of dichloromethane were added. The organic phase was collected and washed with water (3 x 20 mL). The organic phase was then dried over anhydrous magnesium sulfate and filtered. The solvent was reduced to few mL, filtered through a 0.2 μm PTFE membrane, and then diethyl ether was added to cause the precipitation of the pure complex as a yellow solid. The solid was filtered and washed with diethyl ether.

fac-Mn(phen)(CO)₃1

Yield 60 mg (90%). Elemental analysis for C₂₂H₁₃MnN₆O₃: calculated C 56.90, H 2.82, N 18.10; found C 56.68, H 2.55, N 17.83. ν_{\max} (ATR)/cm⁻¹: 2035 (s) (CO), 1939 (s) (2 x CO). ¹H NMR (δ , ppm, Acetone-d₆): 9.73 (2H, dd, ³J_{H-H} = 4.8 Hz, ⁴J_{H-H} = 1.2 Hz, H₄), 8.84 (2H, dd, ³J_{H-H} = 8.4 Hz, ⁴J_{H-H} = 1.2 Hz, H₂), 8.23 (2H, s, H₅), 8.14 (2H, dd, ³J_{H-H} = 8.4 Hz, ³J_{H-H} = 4.8 Hz, H₃), 7.68-7.66 (2H, m, H₆), 7.25-7.16 (3H, m, H₆). ¹³C NMR (δ , ppm, Acetone-d₆): 164.00, 155.22, 148.00, 139.07, 131.81, 130.79, 129.02, 128.60, 128.06, 126.71, 126.55. HR-ESI (*m/z*): calculated 465.0502 (C₂₂H₁₃MnN₆O₃, [M+H]⁺) found 465.0480. Crystals suitable for X-ray analysis were grown via evaporation of a solution of dichloromethane containing the complex.

fac-Mn(phen)(CO)₃2

Yield 42 mg (74 %). Elemental analysis for C₂₁H₁₂MnN₇O₃: calculated C 54.20, H 2.60, N 21.07; found C 53.87, H 2.23, N 20.66. ν_{\max} (ATR)/cm⁻¹: 2036 (s) (CO), 1941 (s) (2 x CO). ¹H NMR (δ , ppm, Acetone-d₆): 9.74 (2H, dd, ³J_{H-H} = 4.8 Hz, ⁴J_{H-H} = 1.2 Hz, H₄), 8.85 (2H, dd, ³J_{H-H} = 8.4 Hz, ⁴J_{H-H} = 1.2 Hz, H₂), 8.79 (1H, s, H₅), 8.39 (1H, d, ³J_{H-H} = 4.4 Hz, H₇), 8.24 (2H, s, H₁), 8.14 (2H, dd, ³J_{H-H} = 8.4 Hz, ³J_{H-H} = 4.8 Hz, H₃), 7.94 (1H, dd, ³J_{H-H} = 6.4 Hz, ⁴J_{H-H} = 1.6 Hz, H₉), 7.23 (1H, dd, ³J_{H-H} = 8.0 Hz, ³J_{H-H} = 4.8 Hz, H₈). ¹³C NMR (δ , ppm, Acetone-d₆): 161.79, 155.28, 149.87, 148.02, 147.96, 139.15, 133.30, 130.82, 128.09, 127.39, 126.77, 124.16. HR-ESI (*m/z*): calculated 466.0455 (C₂₁H₁₂MnN₇O₃, [M+H]⁺) found 466.0436. Crystals suitable for X-ray analysis were grown via vapour diffusion of petroleum spirits (40-60 °C) into a solution of dichloromethane containing the complex.

fac-Mn(phen)(CO)₃3

Yield 36 mg (66 %). Elemental analysis for C₂₁H₁₂MnN₇O₃: calculated C 54.20, H 2.60, N 21.07; found C 54.06, H 2.34, N 20.86. ν_{\max} (ATR)/cm⁻¹: 2036 (s) (CO), 1941 (s) (2 x CO). ¹H NMR (δ , ppm, Acetone-d₆): 9.74 (2H, dd, ³J_{H-H} = 5.2 Hz, ⁴J_{H-H} = 1.2 Hz, H₄), 8.86 (2H, dd, ³J_{H-H} = 8.4 Hz, ⁴J_{H-H} = 1.2 Hz, H₂), 8.44 (2H, d, ³J_{H-H} = 4.8 Hz, H₆), 8.24 (2H, s, H₁), 8.14 (2H, dd, ³J_{H-H} = 8.4 Hz, ³J_{H-H} = 5.2 Hz, H₃), 7.54 (2H, d, ³J_{H-H} = 5.2 Hz, H₅). ¹³C NMR (δ , ppm, Acetone-d₆): 162.29, 155.29, 151.10, 147.98, 139.18,

FULL PAPER

138.49, 130.83, 128.10, 126.78, 120.77. HR-ESI (m/z): calculated 466.0455 ($C_{21}H_{12}MnN_7O_3$, $[M+H]^+$) found 466.0433. Crystals suitable for X-ray analysis were grown via vapour diffusion of petroleum spirits (40–60 °C) into a solution of dichloromethane containing the complex.

fac-Mn(phen)(CO)₃4

Yield 40 mg (63 %). Elemental analysis for $C_{23}H_{12}MnN_7O_3$: calculated C 56.45, H 2.47, N 20.04; found C 56.63, H 2.32, N 20.05. ν_{max} (ATR)/ cm^{-1} : 2036 (s) (CO), 1942 (s) (2 x CO). 1H NMR (δ , ppm, Acetone- d_6): 9.74 (2H, dd, $^3J_{H-H} = 5.2$ Hz, $^4J_{H-H} = 0.8$ Hz, H₄), 8.86 (2H, dd, $^3J_{H-H} = 8.4$ Hz, $^4J_{H-H} = 0.8$ Hz, H₂), 8.24 (2H, s, H₁), 8.14 (2H, dd, $^3J_{H-H} = 8.0$ Hz, $^3J_{H-H} = 1.2$ Hz, H₃), 7.84 (2H, d, $^3J_{H-H} = 8.4$ Hz, H₆), 7.65 (2H, d, $^3J_{H-H} = 8.4$ Hz, H₅). ^{13}C NMR (δ , ppm, Acetone- d_6): 162.82, 155.31, 147.96, 139.19, 135.80, 133.16, 130.83, 128.11, 127.03, 126.80, 119.37, 111.96. HR-ESI (m/z): calculated 490.0455 ($C_{23}H_{12}MnN_7O_3$, $[M+H]^+$) found 490.0437. Crystals suitable for X-ray analysis were grown via vapour diffusion of petroleum spirits (40–60 °C) into a solution of dichloromethane containing the complex.

fac-Mn(phen)(CO)₃5

Yield 46 mg (39%). Elemental analysis for $C_{23}H_{13}MnN_6O_4$: calculated C 56.11, H 2.66, N 17.07; found C 55.77, H 2.47, N 16.92. ν_{max} (ATR)/ cm^{-1} : 2036 (s) (CO), 1942 (s) (2 x CO). 1H NMR (δ , ppm, Acetone- d_6): 9.96 (1H, s, H₇), 9.75 (2H, dd, $^3J_{H-H} = 4.8$ Hz, $^4J_{H-H} = 1.2$ Hz, H₄), 8.86 (2H, dd, $^3J_{H-H} = 8.4$ Hz, $^4J_{H-H} = 1.2$ Hz, H₂), 8.24 (2H, s, H₁), 8.15 (2H, dd, $^3J_{H-H} = 8.4$ Hz, $^3J_{H-H} = 5.2$ Hz, H₃), 7.89–7.87 (2H, m, H₆'), 7.81–7.79 (2H, m, H₅). ^{13}C NMR (δ , ppm, Acetone- d_6): 192.36, 163.26, 155.30, 148.00, 139.16, 137.11, 136.96, 130.84, 130.51, 128.10, 126.89, 126.78. HR-ESI (m/z): calculated 493.0452 ($C_{23}H_{13}MnN_6O_4$, $[M+H]^+$) found 493.0429. Crystals suitable for X-ray analysis were grown via vapour diffusion of ether into a solution of dichloromethane containing the complex.

fac-Mn(batho)(CO)₃1

Yield 52 mg (79%). Elemental analysis for $C_{36}H_{25}MnN_6O_3$: calculated C 67.08, H 3.91, N 13.04; found C 66.80, H 3.70, N 13.04. ν_{max} (ATR)/ cm^{-1} : 2030 (s) (CO), 1932 (s) (2 x CO). 1H NMR (δ , ppm, Acetone- d_6): 7.99 (2H, s, H₁'), 7.88 (2H, s, H₅'), 7.74–7.71 (2H, m, H₇'), 7.65–7.60 (10H, m, H_{2,3,4}'), 7.28–7.21 (3H, m, H_{8,9}') 3.55 (6H, s, H₆'). ^{13}C NMR (δ , ppm, DMSO- d_6): 164.09, 162.54, 149.35, 147.85, 135.49, 129.70, 129.61, 129.48, 129.00, 128.53, 128.29, 127.14, 125.41, 125.35, 123.72, 29.08. HR-ESI (m/z): calculated 645.1441 ($C_{36}H_{25}MnN_6O_3$, $[M+H]^+$) found 645.1428.

fac-Mn(batho)(CO)₃2

Yield 35 mg (63%). Elemental analysis for $C_{35}H_{24}MnN_7O_3 \cdot 0.2CH_2Cl_2$: calculated C 63.81, H 3.71, N 14.80; found C 64.03, H 3.50, N 14.79. ν_{max} (ATR)/ cm^{-1} : 2031 (s) (CO), 1934 (s) (2 x CO). (δ , ppm, Acetone- d_6): 8.88 (1H, d, $^4J_{H-H} = 1.2$ Hz, H₇'), 8.43 (1H, dd, $^3J_{H-H} = 4.8$ Hz, $^4J_{H-H} = 1.6$ Hz, H₉) 8.01–7.98 (3H, m, H_{1,11}'), 7.89 (2H, s, H₅'), 7.65–7.59 (10H, m, H_{2,3,4}'), 7.27 (1H, dd, $^3J_{H-H} = 8.4$ Hz, $^3J_{H-H} = 4.8$ Hz, H₁₀'), 3.56 (6H, s, H₆'). ^{13}C NMR (δ , ppm, DMSO- d_6): 164.15, 160.35, 149.38, 147.82, 147.63, 146.45, 135.47, 132.63, 129.60, 129.49, 128.99, 128.69, 127.20, 125.47, 125.36, 123.73, 29.11. HR-ESI (m/z): calculated 646.1407 ($C_{23}H_{13}MnN_6O_4$, $[M+H]^+$) found 646.1381.

fac-Mn(batho)(CO)₃3

Yield 37 mg (64%). Elemental analysis for $C_{35}H_{24}MnN_7O_3$: calculated C 65.11, H 3.75, N 15.19; found C 65.17, H 3.56, N 14.95. ν_{max} (ATR)/ cm^{-1} :

2031 (s) (CO), 1934 (s) (2 x CO). 1H NMR (δ , ppm, Acetone- d_6): 8.48 (2H, d, $J = 3.6$ Hz, H₈), 8.00 (2H, s, H₁'), 7.89 (2H, s, H₅'), 7.65–7.59 (12H, m, H_{2,3,4,6}'), 3.55 (6H, s, H₆'). ^{13}C NMR (δ , ppm, DMSO- d_6): 164.19, 160.88, 150.21, 149.44, 147.81, 136.50, 135.47, 129.63, 129.53, 129.03, 127.23, 125.38, 123.77, 119.69, 29.12. HR-ESI (m/z): calculated 646.1394 ($C_{35}H_{24}MnN_7O_3$, $[M+H]^+$) found 646.1379.

fac-Mn(batho)(CO)₃4

Yield 41 mg (68%). Elemental analysis for $C_{37}H_{24}MnN_7O_3$: calculated C 66.37, H 3.61, N 14.64; found C 66.36, H 3.52, N 14.42. ν_{max} (ATR)/ cm^{-1} : 2031 (s) (CO), 1934 (s) (2 x CO). 1H NMR (δ , ppm, Acetone- d_6): 8.00 (2H, s, H₁'), 7.90–7.88 (4H, m, H_{5,7}'), 7.68 (2H, dd, 1H, dd, $^3J_{H-H} = 5.6$ Hz, $^4J_{H-H} = 1.6$ Hz, H₈'), 7.64–7.60 (10H, m, H_{2,3,4}'), 3.55 (6H, s, H₆'). ^{13}C NMR (δ , ppm, DMSO- d_6): 164.19, 161.47, 149.44, 147.80, 135.46, 133.80, 132.80, 129.63, 129.53, 129.04, 127.23, 125.95, 125.38, 123.77, 118.7, 110.67, 29.13. HR-ESI (m/z): calculated 670.1394 ($C_{37}H_{24}MnN_7O_3$, $[M+H]^+$) found 670.1386.

fac-Mn(batho)(CO)₃5

Yield 45 mg (73%). Elemental analysis for $C_{37}H_{25}MnN_6O_4$: calculated C 66.07, H 3.75, N 12.49; found C 66.32, H 3.81, N 12.41. ν_{max} (ATR)/ cm^{-1} : 2031 (s) (CO), 1934 (s) (2 x CO). 1H NMR (δ , ppm, Acetone- d_6): 9.98 (1H, s, H₉'), 8.00 (2H, s, H₁'), 7.92 (2H, d, $^3J_{H-H} = 8.4$ Hz, H₈'), 7.89 (2H, s, H₅'), 7.83 (2H, d, $^3J_{H-H} = 8.4$ Hz, H₇'), 7.65–7.61 (10H, m, H_{2,3,4}'), 3.56 (6H, s, H₆'). ^{13}C NMR (δ , ppm, DMSO- d_6): 192.63, 164.24, 161.90, 149.49, 147.91, 135.82, 135.52, 134.99, 130.10, 129.68, 129.59, 129.09, 127.24, 125.91, 125.43, 123.80, 29.17. HR-ESI (m/z): calculated 673.1391 ($C_{37}H_{25}MnN_6O_4$, $[M+H]^+$) found 673.1381.

X-ray diffraction analysis

All crystals were grown via the diffusion of petroleum spirits into dichloromethane. Crystallographic data for the structures were collected at 100(2) K on either an Oxford Diffraction Xcalibur or Gemini diffractometer. Following Lp, and absorption corrections, and solution by direct methods, the structures were refined against F^2 with full-matrix least squares using the program SHELXL-2014.9.^[49] Anisotropic displacement parameters were employed for the non-hydrogen atoms. All hydrogen atoms were added at calculated positions and refined by use of a riding model with isotropic displacement parameters based on those of the parent atom. Crystallographic data for the structures reported in this paper can be found in the Supporting Information and have been deposited at the Cambridge Crystallographic Data Centre. CCDC numbers are given below. Copies of the data can be obtained free of charge via <https://www.ccdc.cam.ac.uk/structures/>, or from the Cambridge Crystallographic Data Centre, 12 Union Road, Cambridge CB2 1EZ, U.KCB21EZ, UK (fax +441223336033; email deposit@ccdc.cam.ac.uk).

Mn(phen)(CO)₃1, $C_{22}H_{13}MnN_6O_3$, $M = 464.32$, $0.168 \times 0.145 \times 0.102$ mm³, triclinic, space group $P1\bar{1}$, $a = 9.2137(4)$, $b = 9.3093(5)$, $c = 12.8795(7)$ Å, $\alpha = 106.306(4)$, $\beta = 96.016(4)$, $\gamma = 109.134(4)^\circ$, $V = 977.82(9)$ Å³, $Z = 2$, $D_c = 1.577$ g/cm³, $\mu = 0.715$ mm⁻¹. $\lambda = 0.71073$ Å, $T = 100(2)$ K, $2\theta_{max} = 65.2^\circ$, 12385 reflections collected, 6444 unique ($R_{int} = 0.0337$). Final $Goof = 1.000$, $R1 = 0.0431$, $wR2 = 0.0918$, R indices based on 5129 reflections with $I > 2\sigma(I)$, $|\Delta\rho|_{max} = 0.50(8)$ e Å⁻³, 289 parameters, 0 restraints. CCDC number 1938962.

Mn(phen)(CO)₃2, $C_{21}H_{12}MnN_7O_3$, $M = 465.32$, $0.224 \times 0.188 \times 0.143$ mm³, triclinic, space group $P1\bar{1}$, $a = 9.1185(3)$, $b = 9.2141(3)$, $c = 12.7940(4)$ Å, $\alpha = 95.906(3)$, $\beta = 104.413(3)$, $\gamma = 108.911(3)^\circ$, $V = 964.94(6)$ Å³, $Z = 2$, $D_c = 1.601$ g/cm³, $\mu = 0.726$ mm⁻¹. $\lambda = 0.71073$ Å, $T = 100(2)$ K, $2\theta_{max} = 64.6^\circ$,

FULL PAPER

20219 reflections collected, 6405 unique ($R_{\text{int}} = 0.0326$). Final $\text{Goof} = 1.066$, $R1 = 0.0386$, $wR2 = 0.0951$, R indices based on 5475 reflections with $I > 2\sigma(I)$, $|\Delta\rho|_{\text{max}} = 0.62(8) \text{ e } \text{Å}^{-3}$, 289 parameters, 0 restraints. CCDC number 1938963

$\text{Mn}(\text{phen})(\text{CO})_3\mathbf{3}$, $\text{C}_{21}\text{H}_{12}\text{MnN}_7\text{O}_3$, $M = 465.32$, $0.183 \times 0.134 \times 0.062 \text{ mm}^3$, monoclinic, space group $C2/c$, $a = 20.0296(8)$, $b = 8.2582(3)$, $c = 25.1697(14) \text{ Å}$, $\beta = 107.279(5)^\circ$, $V = 3975.4(3) \text{ Å}^3$, $Z = 8$, $D_c = 1.555 \text{ g/cm}^3$, $\mu = 5.759 \text{ mm}^{-1}$. $\lambda = 1.54184 \text{ Å}$, $T = 100(2) \text{ K}$, $2\theta_{\text{max}} = 134.6^\circ$, 15582 reflections collected, 3530 unique ($R_{\text{int}} = 0.0598$). Final $\text{Goof} = 1.055$, $R1 = 0.0468$, $wR2 = 0.1267$, R indices based on 3109 reflections with $I > 2\sigma(I)$, $|\Delta\rho|_{\text{max}} = 0.51(7) \text{ e } \text{Å}^{-3}$, 289 parameters, 0 restraints. CCDC number 1938964.

$\text{Mn}(\text{phen})(\text{CO})_3\mathbf{4}$, $\text{C}_{23}\text{H}_{12}\text{MnN}_7\text{O}_3 \cdot 3/4(\text{CH}_2\text{Cl}_2)$, $M = 553.03$, $0.646 \times 0.133 \times 0.042 \text{ mm}^3$, monoclinic, space group $C2/c$, $a = 22.4035(6)$, $b = 17.2137(4)$, $c = 12.7060(2) \text{ Å}$, $\beta = 91.659(2)^\circ$, $V = 4897.98(19) \text{ Å}^3$, $Z = 8$, $D_c = 1.500 \text{ g/cm}^3$, $\mu = 0.744 \text{ mm}^{-1}$. $\lambda = 0.71073 \text{ Å}$, $T = 100(2) \text{ K}$, $2\theta_{\text{max}} = 64.2^\circ$, 27473 reflections collected, 8088 unique ($R_{\text{int}} = 0.0355$). Final $\text{Goof} = 1.055$, $R1 = 0.0605$, $wR2 = 0.1474$, R indices based on 6603 reflections with $I > 2\sigma(I)$, $|\Delta\rho|_{\text{max}} = 1.36(9) \text{ e } \text{Å}^{-3}$, 363 parameters, 16 restraints. CCDC number 1938965.

$\text{Mn}(\text{phen})(\text{CO})_3\mathbf{5}$, $\text{C}_{23}\text{H}_{13}\text{MnN}_6\text{O}_4$, $M = 492.33$, $0.436 \times 0.356 \times 0.093 \text{ mm}^3$, monoclinic, space group $P2_1/n$, $a = 9.4795(2)$, $b = 10.9716(2)$, $c = 20.6393(4) \text{ Å}$, $\beta = 97.321(2)^\circ$, $V = 2129.10(7) \text{ Å}^3$, $Z = 4$, $D_c = 1.536 \text{ g/cm}^3$, $\mu = 0.665 \text{ mm}^{-1}$. $\lambda = 0.71073 \text{ Å}$, $T = 100(2) \text{ K}$, $2\theta_{\text{max}} = 65.4^\circ$, 45622 reflections collected, 7422 unique ($R_{\text{int}} = 0.0330$). Final $\text{Goof} = 1.001$, $R1 = 0.0364$, $wR2 = 0.0977$, R indices based on 6273 reflections with $I > 2\sigma(I)$, $|\Delta\rho|_{\text{max}} = 0.45(7) \text{ e } \text{Å}^{-3}$, 307 parameters, 0 restraints. CCDC number 1938966.

References

- [1] R. Motterlini, B. E. Mann, R. Foresti, *Expert. Opin. Investig. Drugs* **2005**, *14*, 1305-1318.
- [2] T. R. Johnson, B. E. Mann, J. E. Clark, R. Foresti, C. J. Green, R. Motterlini, *Angew. Chem. Int. Ed.* **2003**, *42*, 3722-3729.
- [3] B. E. Mann, *Organometallics* **2012**, *31*, 5728-5735.
- [4] S. W. Ryter, J. Alam, A. M. K. Choi, *Physiol. Rev.* **2006**, *86*, 583-650.
- [5] K. Schmidt, M. Jung, R. Keilitz, B. Schnurr, R. Gust, *Inorganica Chim. Acta* **2000**, *306*, 6-16.
- [6] R. Motterlini, B. Haas, R. Foresti, *Med. Gas Res.* **2012**, *2*, 28-28.
- [7] F. Amersi, X. D. Shen, D. Anselmo, J. Melinek, S. Iyer, D. J. Southard, M. Katori, H. D. Volk, R. W. Busuttill, R. Buelow, J. W. Kupiec-Weglinski, *Hepatology* **2002**, *35*, 815-823.
- [8] K. Sato, J. Balla, L. Otterbein, R. N. Smith, S. Brouard, Y. Lin, E. Csizmadia, J. Sevigny, S. C. Robson, G. Vercellotti, A. M. Choi, F. H. Bach, M. P. Soares, *J. Immunol.* **2001**, *166*, 4185.
- [9] E. O. Leo, H. B. Fritz, A. Jawed, S. Miguel, L. Hong Tao, W. Mark, J. D. Roger, A. F. Richard, M. K. C. Augustine, *Nat. Med.* **2000**, *6*, 422.
- [10] S. P. Gaine, G. Booth, L. Otterbein, N. A. Flavahan, A. M. K. Choi, C. M. Wiener, *J. Vas. Res.* **1999**, *36*, 114-119.
- [11] M. A. Gentile, *Respir. Care* **2011**, *56*, 1341-1357.
- [12] J. Boczkowski, J. J. Poderoso, R. Motterlini, *Trends Biochem. Sci.* **2006**, *31*, 614-621.
- [13] S. García-Gallego, G. J. L. Bernardes, *Angew. Chem. Int. Ed.* **2014**, *53*, 9712-9721.
- [14] R. Motterlini, J. E. Clark, R. Foresti, P. Sarathchandra, B. E. Mann, C. J. Green, *Circ. Res.* **2002**, *90*, E17-24.
- [15] J. Jimenez, I. Chakraborty, S. J. Carrington, P. K. Mascharak, *Dalton Trans.* **2016**, *45*, 13204-13213.
- [16] I. Chakraborty, S. J. Carrington, P. K. Mascharak, *Acc. Chem. Res.* **2014**, *47*, 2603-2611.
- [17] E. Kottelat, F. Zobi, *Inorganics* **2017**, *5*, 24.
- [18] P. C. Ford, *Coord. Chem. Rev.* **2018**, *376*, 548-564.
- [19] M. A. Wright, J. A. Wright, *Dalton Trans.* **2016**, *45*, 6801-6811.
- [20] T. Slanina, P. Ebej, *Photochem. Photobiol. Sci.* **2018**, *17*, 692-710.
- [21] R. D. Rimmer, A. E. Pierri, P. C. Ford, *Coord. Chem. Rev.* **2012**, *256*, 1509-1519.
- [22] Z. Li, A. E. Pierri, P.-J. Huang, G. Wu, A. V. Iretskii, P. C. Ford, *Inorg. Chem.* **2018**, *57*, 6191-6191.
- [23] B. J. Aucott, J. S. Ward, S. G. Andrew, J. Milani, A. C. Whitwood, J. M. Lynam, A. Parkin, I. J. S. Fairlamb, *Inorg. Chem.* **2017**, *56*, 5431.
- [24] J. Ward, J. Bray, B. Aucott, C. Wagner, N. Pridmore, A. Whitwood, J. Moir, J. Lynam, I. Fairlamb, *Eur. J. Inorg. Chem.* **2016**, *2016*, 5044-5051.
- [25] S. H. C. Askes, G. U. Reddy, R. Wyrwa, S. Bonnet, A. Schiller, *J. Am. Chem. Soc.* **2017**, *139*, 15292.
- [26] R. Mede, S. Gläser, B. Suchland, B. Schowtka, M. Mandel, H. Görls, S. Kriek, A. Schiller, M. Westerhausen, *Inorganics* **2017**, *5*, 8.
- [27] F. Zobi, L. Quaroni, G. Santoro, T. Zlateva, O. Blacque, B. Sarafimov, M. C. Schaub, A. Y. Bogdanova, *J. Med. Chem.* **2013**, *56*, 6719-6731.
- [28] E. Kottelat, A. Ruggi, F. Zobi, *Dalton Trans.* **2016**, *45*, 6920-6927.
- [29] M. V. Werrett, P. J. Wright, P. V. Simpson, P. Raiteri, B. W. Skelton, S. Stagni, A. G. Buckley, P. J. Rigby, M. Massi, *Dalton Trans.* **2015**, *44*, 20636-20647.
- [30] C. A. Bader, R. D. Brooks, Y. S. Ng, A. Sorvina, M. V. Werrett, P. J. Wright, A. G. Anwer, D. A. Brooks, S. Stagni, S. Muzzioli, M. Silberstein, B. W. Skelton, E. M. Goldys, S. E. Plush, T. Shandala, M. Massi, *RSC Adv.* **2014**, *4*, 16345-16351.
- [31] N. Akabar, V. Chaturvedi, G. E. Shillito, B. J. Schwehr, K. C. Gordon, G. S. Huff, J. J. Sutton, B. W. Skelton, A. N. Sobolev, S. Stagni, D. J. Nelson, M. Massi, *Dalton Trans.* **2019**.

FULL PAPER

- [32] C. A. Bader, E. A. Carter, A. Safitri, P. V. Simpson, P. Wright, S. Stagni, M. Massi, P. A. Lay, D. A. Brooks, S. E. Plush, *Mol. Biosyst.* **2016**, *12*, 2064-2068.
- [33] E. O. John, R. D. Willett, B. Scott, R. L. Kirchmeier, J. n. M. Shreeve, *Inorg. Chem.* **1989**, *28*, 893-897.
- [34] J.-M. Lin, B.-S. Huang, Y.-F. Guan, Z.-Q. Liu, D.-Y. Wang, W. Dong, *CrystEngComm* **2009**, *11*, 329.
- [35] Y.-B. Lu, M.-S. Wang, W.-W. Zhou, G. Xu, G.-C. Guo, J.-S. Huang, *Inorg. Chem.* **2008**, *47*, 8935-8942.
- [36] C. Janiak, T. G. Scharmann, K. W. Brzezinka, P. Reich, *Chem. Ber.* **1995**, *128*, 323-328.
- [37] M. V. Werrett, G. S. Huff, S. Muzzioli, V. Fiorini, S. Zacchini, B. W. Skelton, A. Maggiore, J. M. Malicka, M. Cocchi, K. C. Gordon, S. Stagni, M. Massi, *Dalton Trans.* **2015**, *44*, 8379-8393.
- [38] M. V. Werrett, S. Muzzioli, P. J. Wright, A. Palazzi, P. Raiteri, S. Zacchini, M. Massi, S. Stagni, *Inorg. Chem.* **2014**, *53*, 229-243.
- [39] M. V. Werrett, D. Chartrand, J. D. Gale, G. S. Hanan, J. G. Maclellan, M. Massi, S. Muzzioli, P. Raiteri, B. W. Skelton, M. Silberstein, S. Stagni, *Inorg. Chem.* **2011**, *50*, 1229-1241.
- [40] J. Jimenez, I. Chakraborty, P. K. Mascharak, *Eur. J. Inorg. Chem.* **2015**, *2015*, 5021-5026.
- [41] U. Schatzschneider, *Eur. J. Inorg. Chem.* **2010**, 1451-1467.
- [42] J. Betts, C. Nagel, U. Schatzschneider, R. Poole, R. M. La Ragione, *PLoS ONE* **2017**, *12*, e0186359.
- [43] C. Nagel, S. McLean, R. K. Poole, H. Braunschweig, T. Kramer, U. Schatzschneider, *Dalton Trans.* **2014**, *43*, 9986-9997.
- [44] J. S. Ward, R. Morgan, J. M. Lynam, I. J. S. Fairlamb, J. W. B. Moir, *MedChemComm* **2017**, *8*, 346-352.
- [45] N. Rana, H. E. Jesse, M. Tinajero-Trejo, J. A. Butler, J. D. Tarlit, M. L. von und zur Muhlen, C. Nagel, U. Schatzschneider, R. K. Poole, *Microbiology* **2017**, *163*, 1477-1489.
- [46] P. V. Simpson, C. Nagel, H. Bruhn, U. Schatzschneider, *Organometallics* **2015**, *34*, 3809-3815.
- [47] J. S. Ward, J. M. Lynam, J. Moir, I. J. S. Fairlamb, *Chem. Eur. J.* **2014**, *20*, 15061-15068.
- [48] P. Sharrock, *Can. J. Microbiol.* **1985**, *31*, 367-370.
- [49] G. M. Sheldrick, *Acta Cryst. C* **2015**, *71*, 3-8.

WILEY-VCH

Accepted Manuscript